MIT Open Access Articles

Manipulation of multimode squeezing in a coupled waveguide array

Manipulation of multimode squeezing in a coupled waveguide array

S. Rojas-Rojas,[1,2] E. Barriga,[3] C. Muñoz,[3] P. Solano,[4] and C. Hermann-Avigliano[2,5,*]

[1]*Departamento de Física, Universidad de Concepción, 160-C Concepción, Chile*
[2]*Millennium Institute for Research in Optics (MIRO), Concepción, Chile*
[3]*Departamento de Física, Facultad de Ciencias, Universidad de Chile, Santiago, Chile*
[4]*Department of Physics, MIT-Harvard Center for Ultracold Atoms, and Research Laboratory of Electronics,*
Massachusetts Institute of Technology, Cambridge, Massachusetts 02139, USA
[5]*Departamento de Física, Facultad de Ciencias Físicas y Matemáticas, Universidad de Chile, Santiago, Chile*

We present a scheme for generating and manipulating three-mode squeezed states with genuine tripartite entanglement by injecting single-mode squeezed light into an array of coupled optical waveguides. We explore the possibility to selectively generate single-mode squeezing or multimode squeezing at the output of an elliptical waveguide array, determined solely by the input light polarization. We study the effect of losses in the waveguide array and show that quantum correlations and squeezing are preserved for realistic parameters. Our results show that arrays of optical waveguides are suitable platforms for generating multimode quantum light, which could lead to novel applications in quantum metrology.

I. INTRODUCTION

Quantum metrology benefits from quantum resources to enhance measurement sensitivity beyond what is possible in classical systems [1]. Squeezed states are a remarkable example of quantum resources. These are states of light with reduced uncertainty in one of the quadratures of the electric field [2]. Their potential applications in the fields of quantum metrology and quantum information have greatly increased in recent decades [3–6], making possible the detection of gravitational waves with enhanced sensitivity [7].

Squeezed states can be generalized to multiple spatial modes of the electromagnetic field, for which noise reduction below the standard quantum limit (SQL) occurs for a linear combinations of the field's quadratures. Multimode squeezed states have promising applications in multiparameter quantum metrology [8–10], multichannel communication, and multichannel quantum imaging [11–14]. Two-mode squeezed states were recently implemented surpassing the SQL for phase measurements [15]. Three-mode squeezed states were obtained via spontaneous parametric six-wave mixing in an atomic-cavity system [16]. However, the generation and manipulation of multimode-squeezed states remains difficult, partially because it requires highly nonlinear processes. Their practical use presents challenges that would be easier to overcome by the manipulation of quantum light with linear optics.

Periodic optical structures, such as photonic crystals, are promising platforms to manipulate light [17,18]. At low optical power, they behave as linear optical systems that allow for the modification of light propagation. These platforms have been extensively studied in the context of classical optics,

but only recently they have enabled the manipulation of nonclassical light [19–25].

Our research focuses on the theoretical study of squeezed light propagation, control, and manipulation in evanescently coupled waveguide arrays with linear response. We seek to understand how quantum features, such as entanglement and squeezing, propagate in these structures. In particular, we study the propagation of quantum light in linear arrays of two and three waveguides. For the former case, we find a perfect analogy with the well-studied effect of a beam splitter [26]. In the case of a three-waveguide array we find that by injecting three single-mode squeezed states, the field evolves into a three-mode squeezed state with a rather simple experimental scheme. We also show that such evolution generates genuine multipartite entanglement. For specific coupling parameters of the waveguides it is possible to choose the output light to be in a multimode or single-mode squeezed state depending on the input light polarization. We consider the effect of losses in the photonic array in order to evaluate the feasibility of the proposed scheme, finding that squeezing and entanglement between waveguides are well preserved in typical experimental configurations. Our results suggest that photonic waveguide arrays are a reliable platform for creating entanglement and three-mode squeezing, with potential scalability to higher-order multimode quantum states generation. This offers new strategies to control highly nonlinear states of light with linear optics, which can potentially impact the scalability of quantum optics experiment with photonic systems.

The paper is organized as follows. We first study the scenario of two evanescently coupled waveguides in Sec. II, and find that in such optical dimer the propagating state varies from two single-mode squeezed states to a two-mode squeezed state, known in the literature as *two-mode squeezed Gaussons* [26]. We then explore, in Sec. III, the propagation of quantum light in a linear array of three waveguides, or optical

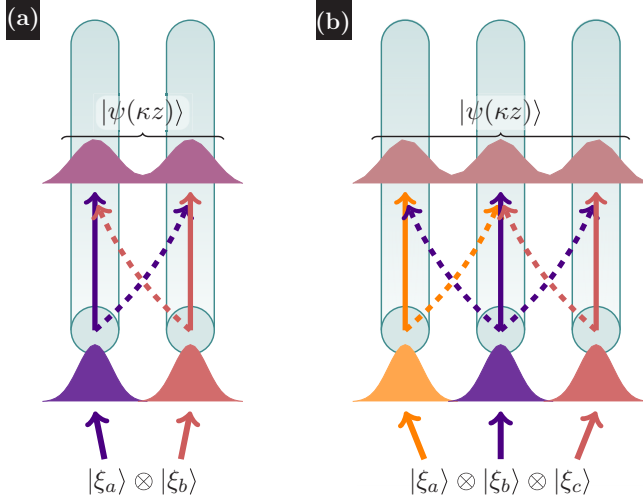*Corresponding author: carla.hermann@uchile.cl

FIG. 1. Squeezing distribution on an optical dimer (a) and trimer (b). Squeezed states defined by their squeezing parameter ξ_i are coupled into the waveguide input. As the state propagates, light is evanescently coupled to neighboring waveguides, as depicted by the dashed arrows. The field evolution results in a multimode correlated state.

trimer. Multipartite entanglement generation and propagation in optical dimers and trimers is studied in Sec. IV. In Sec. V, we show how light polarization serves to manipulate the order of multimodality of the output state. Finally, in Sec. VI, we study the effect of losses in the system and conclude that quantum features are preserved in a realistic scenario. We present our conclusions and remarks in Sec. VII.

II. TWO-MODE SQUEEZING IN AN OPTICAL DIMER

The propagation of light in a linear system with two input and two output ports [see Fig. 1(a)] is described by two modes, a and b, and an evolution operator U that coherently couples both modes as

$$U = \exp\{\gamma a^\dagger b - \gamma^* a b^\dagger\}, \tag{1}$$

with $\gamma = \theta \exp(i\delta)$, where θ and δ are the amplitude and phase of the complex coupling between modes. An initial input state $|\psi_0\rangle$ evolves as it propagates through the system, leading to the state $|\psi\rangle = U^{-1}|\psi_0\rangle$, using the notation from Ref. [26] for simplicity, and considering the fact that U^{-1} differs from U only in the sign of θ.

We study the particular case of an input field with two single-mode squeezed states

$$|\psi_0\rangle = S_a S_b |0, 0\rangle, \tag{2}$$

where the operators S_a and S_b are the single-mode squeezing operators for modes a and b defined by

$$S_j = \exp\left\{\tfrac{1}{2}\left(\xi_j^* a_j^2 - \xi_j (a_j^\dagger)^2\right)\right\}, \tag{3}$$

with $j = a, b$ and their respective squeezing parameter $\xi_j = r_j \exp(i\mu_j)$ a general complex number.

Operator U can be inserted and removed to the left of the vacuum state, meaning that a rotation of the vacuum is again

TABLE I. Conditions to generate two single-mode squeezed states or a sole two-mode squeezed state.

Two single-mode squeezing	
Phases	$2\delta + \mu_a - \mu_b = 2n\pi$
Squeezing strengths	$r_a = r_b$
θ	
Sole two-mode squeezing	
Phases	$2\delta + \mu_a - \mu_b = (2n+1)\pi$
Squeezing strengths	$r_a = r_b$
θ	$\theta = (2m+1)\pi/4$

the vacuum, thus

$$|\psi\rangle = U^{-1} S_a S_b U |0, 0\rangle. \tag{4}$$

As a result, we obtain a general squeezed state $|\psi\rangle$ for two modes

$$|\psi\rangle = \exp\left\{\tfrac{1}{2}(Z_a^* a^2 + Z_b^* b^2 + Z_{ab} b^\dagger a^\dagger - \text{H.c.})\right\}|0, 0\rangle, \tag{5}$$

where Z_a and Z_b are the coefficients of single-mode squeezing, and Z_{ab} corresponds to the coefficient for two-mode squeezing. Depending on the value of these coefficients the state can vary from two single-mode squeezed states ($Z_a \vee Z_b \neq 0$ and $Z_{ab} = 0$) to a sole two-mode squeezed state ($Z_a = Z_b = 0$ and $Z_{ab} \neq 0$). The term sole two-mode squeezing describes the situation where the noise of linear combination of the modes quadratures is below the vacuum noise and all single-mode quadratures noise is equal or higher than vacuum noise. For our particular case of $|\psi_0\rangle$, and using the unitary transformations

$$U^{-1} a U = a \cos\theta + \exp(i\delta) b \sin\theta, \tag{6a}$$

$$U^{-1} b U = b \cos\theta - \exp(-i\delta) a \sin\theta, \tag{6b}$$

the squeezing coefficients are

$$Z_a = \xi_a \cos^2(\theta) + \xi_b \exp(2i\delta) \sin^2(\theta), \tag{7a}$$

$$Z_b = \xi_a \exp(-2i\delta) \sin^2(\theta) + \xi_b \cos^2(\theta), \tag{7b}$$

$$Z_{ab} = -2\cos(\theta)\sin(\theta)[\xi_a \exp(-i\delta) - \xi \exp(i\delta)]. \tag{7c}$$

From these equations we can identify two extreme cases. When $Z_{ab} = 0$ and $Z_a \wedge Z_b \neq 0$ we get two single-mode squeezed states. On the other hand, when $Z_a = Z_b = 0$ and $Z_{ab} \neq 0$ we get a sole two-mode squeezed state. The conditions for realizing both extreme states are summarized in Table I.

The unitary transformations (6a) and (6b) show that a quantum beam splitter is a particular case of the operator U acting on two modes [26].

We are interested in a system of two evanescently coupled optical waveguides, i.e., an optical dimer [see Fig. 1(a)]. The interaction between waveguides in this system is described by the Hamiltonian

$$H = -\hbar\kappa(a^\dagger b + a b^\dagger), \tag{8}$$

where κ is the coupling constant between the waveguides [23,27–29]. We notice that the evolution operator of such a Hamiltonian corresponds to the operator U in the particular case of $\delta = \pi/2$,

$$U = \exp\{i\theta(a^\dagger b + a b^\dagger)\}, \tag{9}$$

with $\theta = \kappa z$, where z is the propagation distance. The light state evolves along the direction of propagation z, hence, κz is the dimensionless parameter controlling the evolution of the state. The squeezing coefficients of the field propagating through the optical dimer are a particular case of Eqs. (7a)–(7c), now in terms of κz:

$$Z_a(\kappa z) = \xi_a \cos^2(\kappa z) - \xi_b \sin^2(\kappa z), \tag{10a}$$

$$Z_b(\kappa z) = -\xi_a \sin^2(\kappa z) + \xi_b \cos^2(\kappa z), \tag{10b}$$

$$Z_{ab}(\kappa z) = 2i(\xi_a + \xi_b)\cos(\kappa z)\sin(\kappa z). \tag{10c}$$

Notice that for particular propagation distances we can obtain either two single-mode squeezed states ($\kappa z = n\pi/2$), or a sole two-mode squeezed state [$\kappa z = (2n+1)\pi/4$ and $\xi_a = \xi_b$].

To study the squeezing evolution in an optical dimer we define the single-mode quadratures for mode a as

$$X_1^a = \frac{1}{2}(e^{-i\phi_0}a + e^{i\phi_0}a^\dagger), \tag{11a}$$

$$X_2^a = \frac{1}{2i}(e^{-i\phi_0}a - e^{i\phi_0}a^\dagger) \tag{11b}$$

and likewise for mode b, where ϕ_0 is the angle that defines the measured quadratures (typically the squeezed and anti-squeezed ones).

Two-mode squeezed states exhibit squeezing in a superposition of quadratures from both modes. The generalized two-mode quadratures are [30]

$$X_1^{2M} = \frac{1}{2^{3/2}}[e^{-i\phi}(a + b) + e^{i\phi}(a^\dagger + b^\dagger)], \tag{12a}$$

$$X_2^{2M} = \frac{1}{2^{3/2}i}[e^{-i\phi}(a + b) - e^{i\phi}(a^\dagger + b^\dagger)], \tag{12b}$$

where ϕ corresponds to the angle where we expect to observe squeezing, in analogy to the single-mode case.

The degree of squeezing is obtained from the variance of the quadratures as

$$S(dB) = 10\log_{10}\left[\frac{\langle(\Delta X)_{sq}^2\rangle}{\langle(\Delta X)_{ch}^2\rangle}\right], \tag{13}$$

where $\langle(\Delta X)_{sq}^2\rangle$ is the variance of the field in the (anti)squeezed quadrature and $\langle(\Delta X)_{ch}^2\rangle = 1/4$ is the variance of a coherent state. The variance of different quadratures can be easily calculated and they are given in Appendix A.

Figure 2 shows the evolution of the input field propagating through an optical dimer. We assume a particular input state $|\psi_0\rangle$, where the squeezing parameters $\xi_a = \xi_b$ are real. In this case, the coefficient $Z_{ab}(\kappa z)$ from Eq. (7c) is always imaginary, meaning that a proper quadrature to measure two-mode squeezing would be $\phi = (2n+1)\pi/4$. In Fig. 2(a) we plot the evolution of the single-mode squeezing coefficients $Z_a = Z_b$ as well as the two-mode squeezing coefficient Z_{ab}. For $\kappa z = 0$, the input state has the same single-mode squeezing in both waveguides and $Z_{ab} = 0$. For $\kappa z = (2n+1)\pi/4$, we get $Z_a = Z_b = 0$ and Z_{ab} is maximum, meaning a sole two-mode squeezed state. Figure 2(b) shows the evolution of the single-mode and generalized two-mode quadrature variances. We notice that for the single-mode quadrature variances the squeezing is lost before $Z_a = Z_b = 0$ because $Z_{ab} \neq 0$ (see
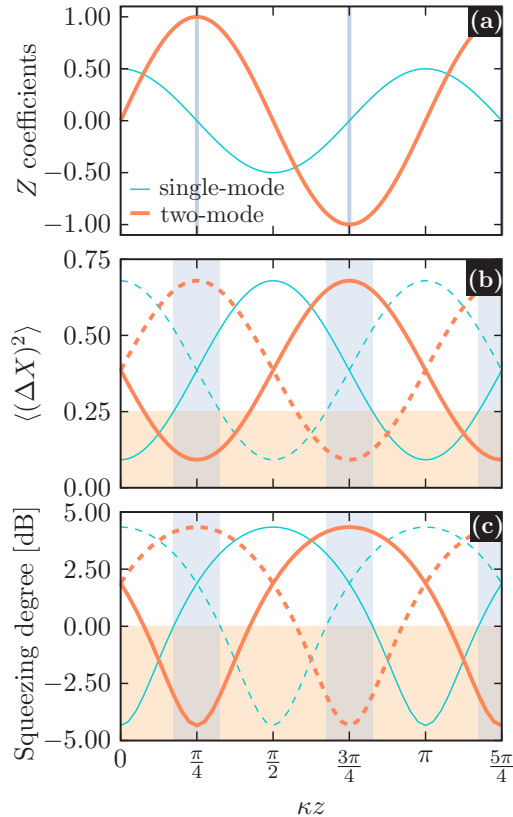

FIG. 2. Evolution of the field along the optical dimer when two single-mode squeezed states with $\xi_a = \xi_b = 0.5$ are injected separately into the waveguides. (a) $Z_a = Z_b$ coefficients (thin cyan curve) and $|Z_{ab}|$ (thick orange curve) as a function of κz. The vertical gray lines show the points where the all the single-mode coefficients (Z) vanish. (b) Variances of the quadratures as a function of κz for both single-mode quadrature variances $\langle(\Delta X_1^{(a,b)})^2\rangle$ and $\langle(\Delta X_2^{(a,b)})^2\rangle$ (thin solid and dashed cyan curves), as well as both two-mode quadrature variances $\langle(\Delta X_1^{2M})^2\rangle$ and $\langle(\Delta X_2^{2M})^2\rangle$ (thick solid and dashed orange curves). (c) Squeezing degree as a function of κz for the same quadratures as in (b). Squeezing is observed when the curves in (b) and (c) are within the orange region. The vertical gray bands in (b) and (c) show the regions where sole two-mode squeezing is observed.

Appendix A for the analytic expressions). This feature is represented by the gray bands in Fig. 2.

The degrees of squeezing of each single-mode squeezed input state are transferred to a sole two-mode squeezed state, and vice versa, as Fig. 2(c) shows. Notice that we can analogously inject a two-mode squeezed state into the optical dimer and get two independent single-mode squeezed states at the output, as shown in detail in Appendix B.

If we inject a single-mode squeezed state only into waveguide mode a, leaving b in the vacuum state, then after a propagation distance of $\kappa z = (2n+1)\pi/2$ all the squeezing is transferred from mode a to b [19]. However, when squeezing is just injected in one of the waveguides, it is impossible to generate a sole two-mode squeezed state.

The transfer of squeezing between modes can be visualized using the Wigner function [31,32], a quasiprobability distribution of the fields in the quadrature space. The Wigner function
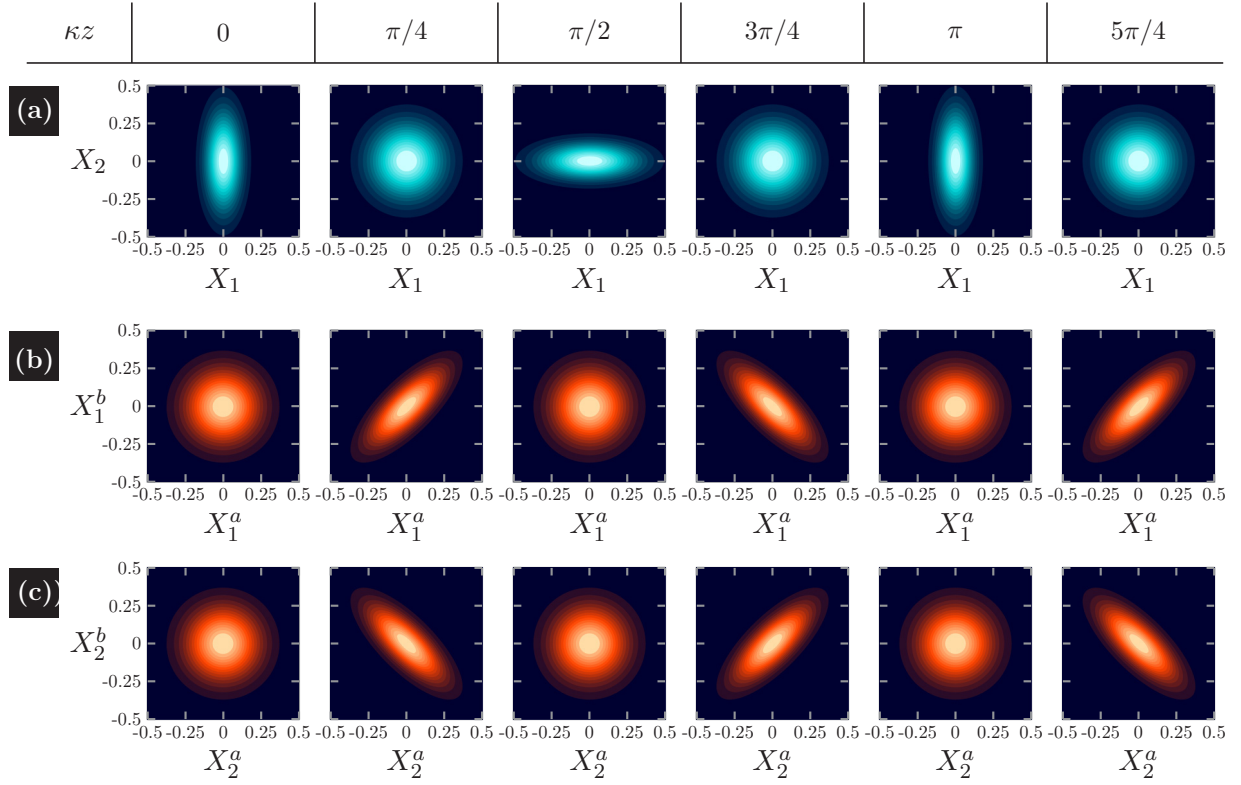
FIG. 3. Evolution of the Wigner function of the reduced single-mode and two-mode states along an optical dimer. (a) Wigner function of the reduced single-mode states on waveguides *a* and *b*. (b) and (c) are the marginal distributions $|\psi(X_1^a, X_1^b)|^2$ and $|\psi(X_2^a, X_2^b)|^2$ of the two-mode Wigner function. The initial state and the color code are the same as Fig. 2.

of a vacuum state gives a symmetric Gaussian distribution, while a squeezed state shows a narrowing of the distribution along a given direction. We compute the Wigner functions for the reduced state of each waveguide, as well as for the two-mode (bipartite) state. The Wigner function of two-mode states W^{2M} is defined by four variables, namely, a pair of quadratures on each mode. In order to make its visualization possible, we compute the marginal distributions of the complete Wigner function, which reflects the correlations of fields propagating through optical array. This gives a quasiprobability distribution as a function of a subset of two out of four modes. We consider the marginal distributions for two pairs of cross-correlated quadratures

$$\left|\psi\left(X_1^a, X_1^b\right)\right|^2 = \int dX_2^a dX_2^b \, W^{2M}\left(X_1^a, X_2^a, X_1^b, X_2^b\right), \quad (14)$$

$$\left|\psi\left(X_2^a, X_2^b\right)\right|^2 = \int dX_1^a dX_1^b \, W^{2M}\left(X_1^a, X_2^a, X_1^b, X_2^b\right). \quad (15)$$

Figure 3 shows the Wigner functions of the single- and the two-mode states, considering the same parameters as in Fig. 2. At the input ($\kappa z = 0$) the single-mode states of each waveguide exhibit a Wigner function squeezed on the X_1 quadratures ($\xi_a = \xi_b$). As the state propagates ($\kappa z = \pi/4$), the single-mode squeezing is lost. In contrast, the Wigner function for the two-mode state is symmetric at the input and, as the state propagates, $|\psi(X_1^a, X_1^b)|^2$ and $|\psi(X_2^a, X_2^b)|^2$ become squeezed, exhibiting correlation and anticorrelation between the cross-correlated quadratures.

III. THREE-MODE SQUEEZING IN AN OPTICAL TRIMER

A linear optical system with three input and three output ports, as Fig. 1(b) shows, is described by three modes *a*, *b*, and *c*, and the evolution operator

$$U_{\rm T} = \exp\{(\alpha^* ab^\dagger - \alpha ba^\dagger + \beta^* bc^\dagger - \beta cb^\dagger)\}, \quad (16)$$

that coherently couples all three modes. $\alpha = \theta_\alpha e^{i\delta_\alpha}$ and $\beta = \theta_\beta e^{i\delta_\beta}$ are complex numbers that characterize the coupling strength between neighboring waveguides.

We study the particular case of injecting a single-mode squeezed states into each input port, $|\phi_0\rangle_{\rm T} = S_a S_b S_c |0, 0, 0\rangle$, with the single-mode squeezing operator defined in Eq. (3), in analogy with Sec. II. Light propagates through the waveguide array evolving into the state

$$|\Psi\rangle_{\rm T} = U_{\rm T}^{-1} S_a S_b S_c U_{\rm T} |0, 0, 0\rangle. \quad (17)$$

After propagation, we obtain a general state with mixed characteristics of single-mode, two-mode, and three-mode squeezing, namely [33],

$$|\Psi\rangle_{\rm T} = \exp\left\{ \tfrac{1}{2}(T_a^* a^2 + T_b^* b^2 + T_c^* c^2 + T_{ab} a^\dagger b^\dagger \right.$$
$$\left. + T_{ac} a^\dagger c^\dagger + T_{bc} b^\dagger c^\dagger - {\rm H.c.}) \right\} |0, 0, 0\rangle. \quad (18)$$

The squeezing parameters T_i and T_{ij} (with $i, j = a, b, c$) have an analogous interpretation as the squeezing Z coefficient in the optical dimer. In the case of $T_a \vee T_b \vee T_c \neq 0$ and $T_{ab} = T_{bc} = T_{ac} = 0$ we have sole single-mode squeezing. If $T_a = T_b = T_c = 0$ and only one $T_{ij} \neq 0$ with the other pairwise coefficients equal to zero, we have sole two-mode squeezing.

Finally, if $T_a = T_b = T_c = 0$ and $T_{ab} \wedge T_{bc} \wedge T_{ac} \neq 0$, we have sole three-mode squeezing. This comes from the definition of multimode squeezing, where the uncertainty of the pairwise sum of quadratures is reduced for all the pairs of modes [33]. As in Sec. II, the term sole three-mode squeezing describes a field where all single-mode quadrature noise is equal or higher than vacuum noise.

The squeezing T coefficients are directly calculated using the rotations

$$U^{-1}aU = \cos^2\left(\frac{\theta}{\sqrt{2}}\right)a + \frac{e^{i\delta}}{\sqrt{2}}\sin(\sqrt{2}\theta)b$$
$$+ e^{2i\delta}\sin^2\left(\frac{\theta}{\sqrt{2}}\right)c, \tag{19a}$$

$$U^{-1}bU = -\frac{1}{\sqrt{2}}e^{-i\delta}\sin(\sqrt{2}\theta)a + \cos(\sqrt{2}\theta)b$$
$$+ \frac{1}{\sqrt{2}}e^{i\delta}\sin(\sqrt{2}\theta)c, \tag{19b}$$

$$U^{-1}cU = e^{-2i\delta}\sin^2\left(\frac{\theta}{\sqrt{2}}\right)a - \frac{1}{\sqrt{2}}e^{-i\delta}\sin(\sqrt{2}\theta)b$$
$$+ \cos^2\left(\frac{\theta}{\sqrt{2}}\right)c, \tag{19c}$$

where we assume equal coupling among waveguides, i.e., $\alpha = \beta$, for simplicity. The most general rotations are detailed in Appendix C.

We study an optical trimer consisting of a linear array of three identical coupled waveguides, as Fig. 1(b) shows. The interaction Hamiltonian of the system is [19,23,27–29]

$$H = -\hbar\kappa(a^\dagger b + ab^\dagger + b^\dagger c + c^\dagger b). \tag{20}$$

The evolution of the light propagating through the waveguides along the z direction is governed by the coupling constant κ. An optical trimer is a particular case of U_T on Eq. (16) for $\delta = \pi/2$. Then, the squeezing T coefficients are

$$T_a = \xi_a \cos^4\left(\frac{\kappa z}{\sqrt{2}}\right) - \xi_b \frac{1}{2}\sin^2(\sqrt{2}\kappa z) + \xi_c \sin^4\left(\frac{\kappa z}{\sqrt{2}}\right),$$

$$T_b = -\xi_a \frac{1}{2}\sin^2(\sqrt{2}\kappa z) + \xi_b \cos^2(\sqrt{2}\kappa z)$$
$$- \xi_c \frac{1}{2}\sin^2(\sqrt{2}\kappa z),$$

$$T_c = \xi_a \sin^4\left(\frac{\kappa z}{\sqrt{2}}\right) - \xi_b \frac{1}{2}\sin^2(\sqrt{2}\kappa z) + \xi_c \cos^4\left(\frac{\kappa z}{\sqrt{2}}\right),$$

$$T_{ab} = i\xi_a\sqrt{2}\sin(\sqrt{2}\kappa z)\cos^2\left(\frac{\kappa z}{\sqrt{2}}\right) + i\xi_b\frac{1}{\sqrt{2}}\sin(2\sqrt{2}\kappa z)$$
$$- i\xi_c\sqrt{2}\sin(\sqrt{2}\kappa z)\sin^2\left(\frac{\kappa z}{\sqrt{2}}\right),$$

$$T_{ac} = \xi_a\frac{1}{2}\sin^2(\sqrt{2}\kappa z) + \xi_b\sin^2(\sqrt{2}\kappa z) + \xi_c\frac{1}{2}\sin^2(\sqrt{2}\kappa z),$$

$$T_{bc} = -i\xi_a\sqrt{2}\sin(\sqrt{2}\kappa z)\sin^2\left(\frac{\kappa z}{\sqrt{2}}\right) + i\xi_b\frac{1}{\sqrt{2}}\sin(2\sqrt{2}\kappa z)$$
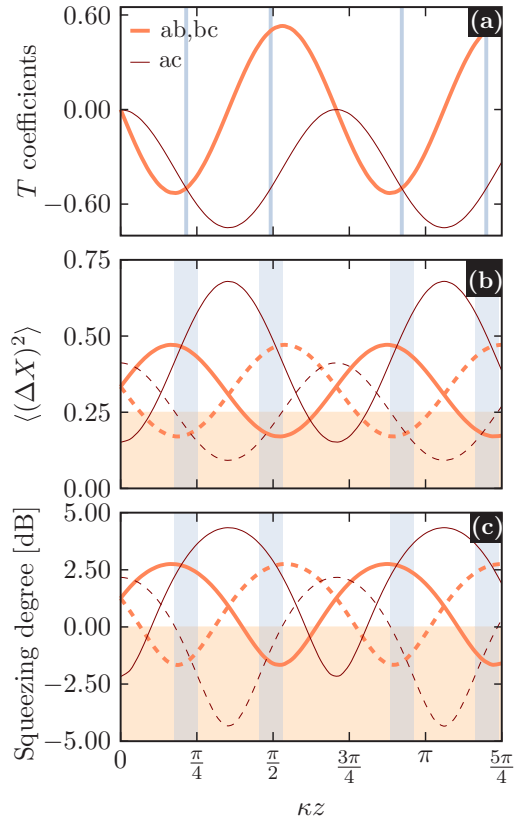$$+ i\xi_c\sqrt{2}\sin(\sqrt{2}\kappa z)\cos^2\left(\frac{\kappa z}{\sqrt{2}}\right). \tag{21}$$

FIG. 4. Evolution of the field along the optical trimer when three single-mode squeezed states, with $\xi_a = \xi_c = 0.25$ and $\xi_b = 0.5$, are injected into the waveguides. (a) Amplitude of the $T_{ab} = T_{bc}$ coefficients (thick orange curve) and the T_{ac} coefficient (thin brown curve) as a function of the normalized propagation distance κz. The vertical gray lines show the points where the all the single-mode coefficients (T_j) vanish. (b) Variances of the quadratures as a function of κz for the two-mode quadrature variances $X_1^{ab} = X_1^{bc}$ and $X_2^{ab} = X_2^{bc}$ (thick solid and dashed orange curves), as well as X_1^{ac} and X_2^{ac} (thin solid and dashed brown curves). (c) Squeezing degree as a function of κz for the same quadratures than in (b). Squeezing is observed when the curves in (b) and (c) are within the orange region. The vertical gray bands in (b) and (c) show the regions where sole three-mode squeezing is observed.

These equations describe a general solution for the propagation of squeezed light through an optical trimer with equal coupling coefficients. Three-mode squeezed states are generated for an input state $|\phi_0\rangle_T$ with real squeezing parameters $\xi_a = \xi_c = \xi_b/2$. Figure 4 shows the evolution of the input field propagating through an optical trimer. Figure 4(a) shows $T_{ab} = T_{bc}$ and T_{ac} as a function of the propagation parameter κz. From Eq. (21) we can easily verify that for $\kappa z = n\pi/\sqrt{2}$, $T_{ab} = T_{ac} = T_{bc} = 0$, as Fig. 4(a) shows, while T_a, T_b, and T_c are different from zero [not shown in Fig. 4(a)]. For $\kappa z = (2n+1)\pi/2\sqrt{2}$, the coefficients T_{ab} and T_{bc} vanish, while T_{ac} does not. However, this is not a sole two-mode squeezed state since T_a, T_b, and T_c are also different from zero. In order to get a sole three-mode squeezed state we need $T_a = T_b = T_c = 0$. This happens for angles $\kappa z_1 = [n\pi + \arctan(\sqrt{2})]/\sqrt{2}$ and $\kappa z_2 = [n\pi - \arctan(\sqrt{2})]/\sqrt{2}$, for the particular case of input states with $\xi_a = \xi_c = \xi_b/2$ [vertical blue lines in Fig. 4(a)].
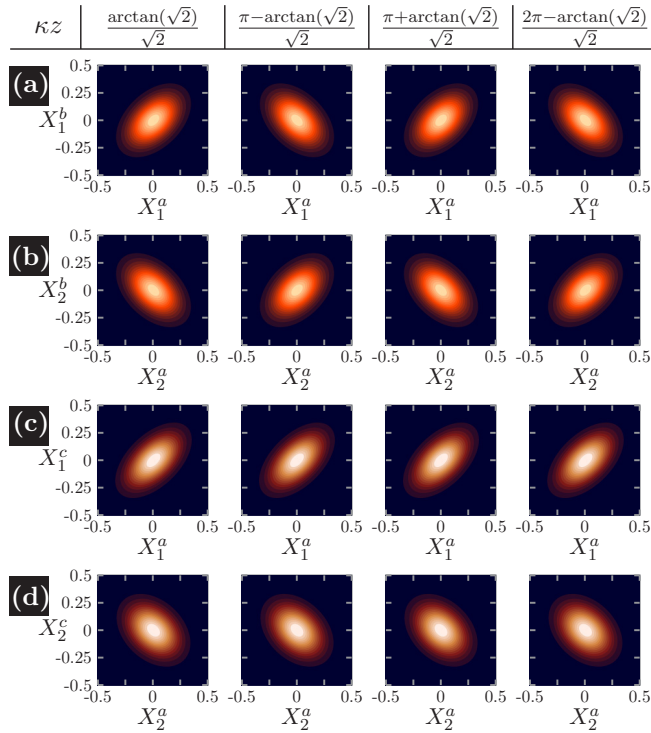
FIG. 5. Evolution of the marginal distributions from the Wigner function of different pairs of modes. (a) Marginal distribution $|\psi(X_1^a, X_1^b)|^2 = |\psi(X_1^b, X_1^c)|^2$. (b) Marginal distribution $|\psi(X_2^a, X_2^b)|^2 = |\psi(X_2^b, X_2^c)|^2$. (c) Marginal distribution $|\psi(X_1^a, X_1^c)|^2$. (d) Marginal distribution $|\psi(X_2^a, X_2^c)|^2$. The initial state and the color code are the same as in Fig. 4.

Figures 4(b) and 4(c) show the evolution of the variances of the generalized two-mode quadratures and the degree of squeezing for each possible pair of modes ab, bc, and ac. Both the variances and the squeezing degree for the combined modes ab and bc are always equal. Sole three-mode squeezing is observed within the gray bands, where single-mode squeezing is absent from all the waveguides, in analogy to Fig. 2 in Sec. II. We notice that a reduction or amplification of noise (relative to vacuum noise) can appear for a particular sum of quadratures when considering two modes with single-mode squeezing [see the brown curves in Figs. 2(b) and 2(c) at $\kappa z = 0$]. This is the result of adding two fields with reduced or increased uncorrelated noise and does not signify a correlation between them. However, when the single-mode squeezing is zero in all modes ($T_a = T_b = T_c = 0$) we can guarantee multimode squeezing with genuine quantum correlation.

We can visualize the evolution of the three-mode squeezed state using the Wigner function following the analysis in Sec. II. Figure 5 shows the marginal distributions of the Wigner function for different combinations of two-mode states. In particular, it shows the Wigner function at the propagation distances κz where squeezing is observed in all the combinations of two modes but not in each individual mode, meaning a sole three-mode squeezed state.

If squeezing is injected only into waveguide a we obtain complete transfer of squeezing from waveguide a to c for $kz = \pi/\sqrt{2}$ [19]. When squeezing is injected just in the

middle waveguide, squeezing is transferred to waveguide a and waveguide c, for $kz = \sqrt{2}\pi/4$. This is a general two-mode squeezed state with $T_a = T_c = -\xi_b/2$ and $T_{ac} = -\xi_b$, such as the state in Eq. (5), while all the other T coefficients vanish.

IV. ENTANGLEMENT GENERATION AND PROPAGATION

Multimode squeezed states show evident cross correlations between quadratures of different modes. However, we cannot assume that these correlations are quantum in nature, i.e., entanglement. Even though squeezing and entanglement are closely related, to the point that two-mode squeezed states can be a physical realization of the ideal two-particle Einstein-Podolsky-Rosen (EPR) state [32], they do not have a direct correspondence. The defining property of an entangled state is its nonseparability, meaning its density matrix cannot be represented as the external product of two density matrices. A particular test for nonseparability, known as the Peres-Horodecki criterion [34,35], tells that a state is nonseparable if the partial transpose of its density matrix has negative eigenvalues.

The Peres-Horodecki criterion can be extended to multipartite continuous-variable states as follows [32,36]. The Wigner function for Gaussian states of N modes is characterized by a correlation matrix $V^{(N)}$, a $2N \times 2N$ matrix with elements defined by

$$V_{ij}^{(N)} = \text{tr}\{\rho \left(\Delta \zeta_i \Delta \zeta_j + \Delta \zeta_j \Delta \zeta_i \right)/2\}, \qquad (22)$$

where $\zeta = (X_1^a X_2^a X_1^b X_2^b \ldots X_1^N X_2^N)$ is a $2N$-dimensional vector operator that contains all the quadrature operators. In the particular case of zero mean value of the quadratures (such as vacuum state) $V_{ij}^{(N)} = \langle (\hat{\zeta}_i \hat{\zeta}_j + \hat{\zeta}_j \hat{\zeta}_i)/2 \rangle$. Under this approach the partial transposition of a continuous-variable state is simply a sign change of the momentum quadrature (X_2) of a subsystem. The partial transpose operation acts on the correlation matrix as $\bar{V}_j^{(N)} = \Gamma_j V^{(N)} \Gamma_j$, where Γ_j are the transposition operator performing the sign change of the X_2 variable in subsystem j. The negative partial transpose criterion for continuous variables says that a separable state satisfies the N-mode uncertainty relation even after partial transposition in site j, i.e.,

$$\bar{V}_j^{(N)} \geqslant \frac{i}{4} \Lambda, \qquad (23)$$

with Λ the $2N \times 2N$ block matrix containing the values of commutators between all the possible pairs of quadratures from every subsystem ($\frac{i}{2}\Lambda_{ij} = [\zeta_i, \zeta_j]$). For example, in a bipartite system,

$$\Lambda = \begin{pmatrix} J & 0 \\ 0 & J \end{pmatrix}, \quad J = \begin{pmatrix} 0 & 1 \\ -1 & 0 \end{pmatrix}.$$

The negative partial transpose criterion for continuous variables is summarized from Eq. (23) as follows: an N-modes state is entangled if ($\bar{V}_j^{(N)} - \frac{i}{4}\Lambda$) has a negative eigenvalue. Figure 6 shows the minimum of the eigenvalues of the operators ($\bar{V}_j^{(N)} - \frac{i}{4}\Lambda$) for the optical dimer (a) and trimer (b), as a function of the propagation distance κz. The input states ($\kappa z = 0$) have a minimum eigenvalue of zero since our initial condition is a product of uncoupled squeezed states. As light
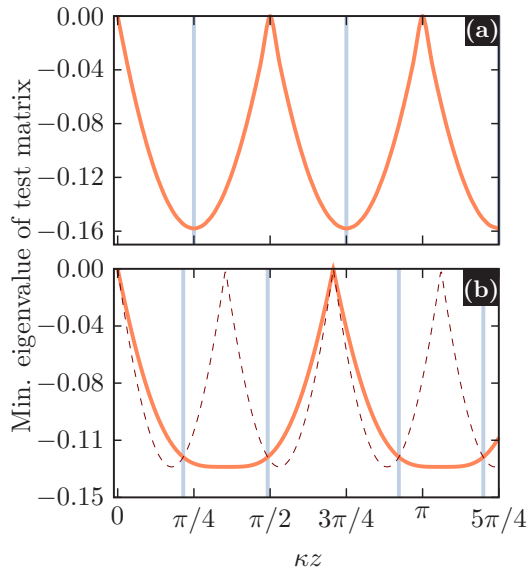
FIG. 6. Entanglement properties of the light propagating through the waveguide arrays (κz). Negative eigenvalues correspond to entangled states. (a) Minimum eigenvalue of the matrix $\bar{V}_j^{(2)} - \frac{i}{4}\Lambda$, for both $j = a, b$. (c) Minimum eigenvalue of matrices $\bar{V}_j^{(3)} - \frac{i}{4}\Lambda$ for $j = a$ and $j = c$ (orange thick curve), and $j = b$ (brown thin dashed curve). The vertical gray lines show the angles where sole two-mode (a) and three-mode (b) squeezing is observed.

propagates through the waveguide array, the minimum eigenvalues become negative, evidencing multimode entanglement, in agreement with the behavior of the squeezing parameters and the Wigner functions (see Figs. 2–5).

We are particularly interested in the case of an optical trimer, where quantum correlations between three-mode continuous variables can be observed. The study of tripartite entanglement for arbitrary dimensions is still a subject of research [37], due to the difficulties to determine how the entanglement is distributed among the parties. To determine the presence of genuine tripartite entanglement, we show the full inseparability of the state. In general, these two concepts are not equivalent; however, for pure states, like the ones studied here, full inseparability implies genuine tripartite entanglement (see Ref. [38] and Supplemental Material in Ref. [39]). In order to verify full inseparability, it is necessary to rule out all the possible partially separable forms, corresponding to all the combinations of bipartite subsystems. From the negative partial transpose criterion for continuous variables we can distinguish the following four scenarios [40]:

$$\text{I.} \quad \bar{V}_a^{(3)} \not\geq \frac{i}{4}\Lambda, \quad \bar{V}_b^{(3)} \not\geq \frac{i}{4}\Lambda, \quad \bar{V}_c^{(3)} \not\geq \frac{i}{4}\Lambda,$$

$$\text{II.} \quad \bar{V}_k^{(3)} \geq \frac{i}{4}\Lambda, \quad \bar{V}_m^{(3)} \not\geq \frac{i}{4}\Lambda, \quad \bar{V}_n^{(3)} \not\geq \frac{i}{4}\Lambda,$$

$$\text{III.} \quad \bar{V}_k^{(3)} \geq \frac{i}{4}\Lambda, \quad \bar{V}_m^{(3)} \geq \frac{i}{4}\Lambda, \quad \bar{V}_n^{(3)} \not\geq \frac{i}{4}\Lambda,$$

$$\text{IV.} \quad \bar{V}_a^{(3)} \geq \frac{i}{4}\Lambda, \quad \bar{V}_b^{(3)} \geq \frac{i}{4}\Lambda, \quad \bar{V}_c^{(3)} \geq \frac{i}{4}\Lambda,$$

where only case I represents full inseparability. Figure 6(b) shows the minimum eigenvalue of $\bar{V}_j^{(3)} - \frac{i}{4}\Lambda$ for $j = a, b, c$.
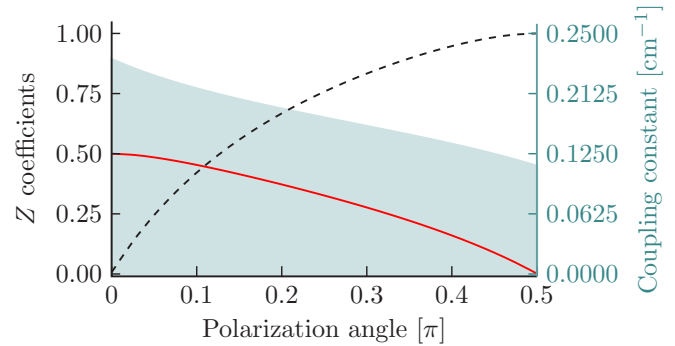

FIG. 7. $Z_a = Z_b$ (solid red curve) and Z_{ab} (dashed black curve) as a function of the input light polarization angle in an optical dimer with elliptical waveguides. The shaded region and the right vertical axis show the range of achievable coupling constants as a function of the polarization angle [42].

As the state propagates through the waveguide array, all the permuted correlation matrix violate the three-mode uncertainty relation and the test matrices have a negative eigenvalue. This means that we observe full inseparability through most of the propagation (case I). At normalized distances $\kappa z = (2n+1)\pi/2\sqrt{2}$ (where coefficients T_{ab} and T_{bc} are exactly zero) we have scenario II, meaning that waveguide b is separable from the bipartite entangled reduced state of waveguides a and c. At points $\kappa z = n\pi/\sqrt{2}$ (where $T_{ab} = T_{bc} = T_{ac} = 0$) we recover the separable state of the input, corresponding to the case IV.

V. SELECTING SQUEEZING MULTIMODALITY BY LIGHT POLARIZATION

Elliptical waveguides allow to tune the coupling constant κ by varying the input light polarization. These are made by a fs-laser-writing fabrication procedure, where the shape of the writing beam and the writing speed are adjusted to create waveguides with an elliptical cross section [41]. Highly elliptical waveguides [42], whose cross sections are $4 \times 12~\mu\text{m}^2$ and separated by 23 μm, can have a ratio between coupling constants for H- and V-polarized light close to 2. The considerable difference between coupling constants suggests that the evolution of a state can be radically different depending upon its polarization.

We compute the evolution of the field through an optical dimer with elliptical waveguides, with tunable coupling constants as a function of the input light polarization angle. Following the mathematical treatment in Sec. II, we assume two single-mode squeezed states of equal squeezing parameter ξ at the input. Figure 7 shows realistic values for the coupling constant as a function of the polarization angle. We compute the Z coefficients for single-mode and two-mode squeezing at the output of the waveguides for a propagation distance $\kappa_H z_{\text{out}} = \pi/2$. Notice how the multimodality of the squeezing varies drastically with the polarization angle. When light is horizontally polarized (0°) the output corresponds to only a single-mode squeezing. At 90°, $|Z_a| = |Z_b| = 0$ and $|Z_{ab}|$ reaches its maximum value. Hence, it is possible to modify the output state from single-mode squeezing to sole

two-mode squeezing, just by tuning the polarization angle of the input linear. This suggests that a dimer built with elliptical waveguides can be used as a powerful tool for controlling and selecting the multimodality of the squeezed light field.

Squeezing tunability as a function of the light polarization may also offer the possibility of creating entanglement between the output light polarization and the order of the multimode squeezing. In this way, the order of the multimode squeezing can be chosen at the output by post-selecting in polarization. The calculation of this effect needs a more complicated mathematical description that will be evaluated in a separate work.

VI. SQUEEZING DEGRADATION IN A LOSSY WAVEGUIDE ARRAY

Optical losses in dielectric media are unavoidable, reducing the degree of squeezing of the propagating light. In general, any type of losses can be modeled with an effective beam splitter, where a fraction of the field is lost at one of the output ports. In such model the transmitted field is scaled by a factor η. The reduction in the squeezing as a function of the losses is given by [30,43]

$$S_{\text{out}} = -\frac{1}{2}\ln\{\eta(z)e^{-2S_{in}} + [1 - \eta(z)]\}, \tag{24}$$

where $S_{\text{in (out)}}$ is the degree of squeezing at the input (output) and $\eta(z)$ is the loss after propagating a distance z. The variable η can represent any type of losses in the system, such as losses by coupling the light into the waveguide or losses during propagation.

Light squeezing, as well as its intensity, is attenuated exponentially as a function of propagation distance, following Beer-Lambert-Bouguer law. Assuming that losses affect equally all waveguides, the evolution of the state remains unchanged except for an overall reduction of the correlations as light attenuates. Figure 8 shows the degradation of the degree of squeezing as a function of the propagation distance for an optical dimer and trimer. In both cases, squeezing is preserved despite of degradation. For realistic parameters it is possible to observe several oscillations of the degree of squeezing before it is completely attenuated.

The degradation of squeezing can also be calculated by solving the master equation including losses, where photon absorption is described as an amplitude damping channel [27,44]. With this approach we find results equivalent to Fig. 8. However, Eq. (24) also allows for easily including the effect of injection losses when coupling free-space propagation light into the waveguide. Injection losses are not considered in Fig. 8, but they will contribute to an overall reduction of the degree of squeezing. Nonetheless, we emphasize that multimode squeezing in a coupled waveguide array is preserved under common mechanism of losses.

VII. CONCLUSIONS AND PERSPECTIVES

We propose a method for the generation and manipulation of two- and three-mode squeezed states via the injection of single-mode squeezed light in a linear array of two and three evanescently coupled waveguides. We observe that the squeezing evolves as it propagates through the waveguides
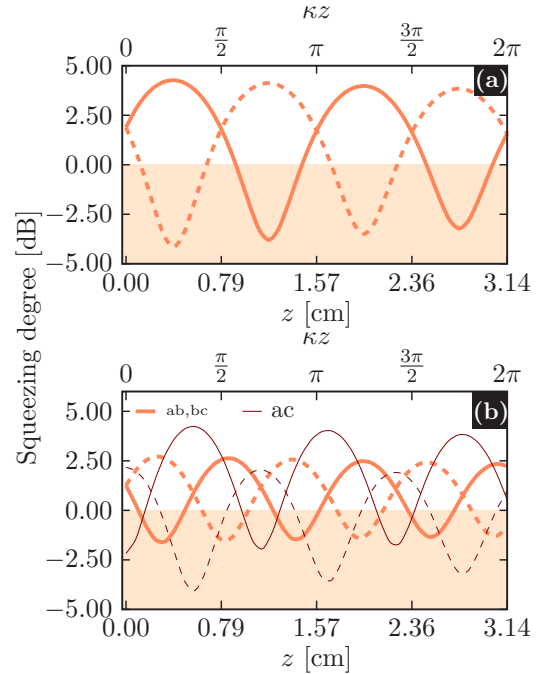

FIG. 8. Degree of squeezing versus propagation distance. (a) Optical dimer for an input of two single-mode squeezed states with squeezing parameter $\xi_a = \xi_b = 0.5$. The degree of squeezing is shown for the two-mode quadratures $\langle(\Delta X_1^{2M})^2\rangle$ and $\langle(\Delta X_2^{2M})^2\rangle$ (solid and dashed orange curves). (b) Optical trimer for an input state of three vacuum-squeezed states with squeezing parameter $\xi_a = \xi_c = 0.25$ and $\xi_b = 0.5$. The degree of squeezing is shown for the two-mode quadratures $X_1^{ab} = X_1^{bc}$ and $X_2^{ab} = X_2^{bc}$ (solid and dashed orange curves), as well as X_1^{ac} and X_2^{ac} (solid and dashed brown curves). For both figures the losses are 0.3 dB/cm [45] and the evanescent coupling coefficient is $\kappa = 2$ cm^{-1} [41], which can be understood as an evolution of κz from 0 to 2π. Squeezing is observed when the curves are within the orange region.

exchanging the roles of single-mode and multimode squeezing. During light propagation, the waveguide array generates genuine multipartite entanglement. This offers a way to control the quantum nonlinear property of multimode squeezing only using a linear optics element. We show that the order of multimode squeezing at the output of the system can be selected by choosing the polarization angle of the input light, offering a novel tuning knob for controlling squeezing. The parameters' tunability in an array of waveguides with linear response facilitates the engineering of quantum states of light. A review of realistic parameters for optical losses in a system of coupled waveguides shows that a significant degree of squeezing is preserved during propagation.

Waveguide arrays are a suitable platform to manipulate quantum light properties, such as squeezing and entanglement. They open new possibilities to generate and control multimode squeezing, with the potential to generate N-mode squeezed states with N coupled waveguides. Multiple modes can be used as multiple probes that measure different local conditions, presenting a problem of multivariables estimation. It is known that quantum correlations can improve the sensitivity of such scenario, making multimode squeezing a

potential resource to improve multiple-variable measurements. By combining quantum light with photonic crystals, our results bring different insights and tools in the fields of quantum information and precision measurement.

APPENDIX A: VARIANCE OF THE FIELD IN AN OPTICAL DIMER

We notice in Fig. 2(b) that for the single-mode quadrature variances, the squeezing is lost before $Z_a = Z_b = 0$ because $Z_{ab} \neq 0$. We can evaluate this using the following transformations ($\xi_i = r_i \exp i\mu_i$):

$$
\begin{aligned}
S_a^{-1} & S_b^{-1} U a U^{-1} S_b S_a \\
&= [a \cosh(r_a) - a^\dagger e^{i\mu_a} \sinh(r_a)] \cos(\kappa z) \\
&\quad - i[b \cosh(r_b) - b^\dagger e^{i\mu_b} \sinh(r_b)] \sin(\kappa z),
\end{aligned} \quad \text{(A1a)}
$$

$$
\begin{aligned}
S_a^{-1} & S_b^{-1} U b U^{-1} S_b S_a \\
&= i[a^\dagger e^{i\mu_a} \sinh(r_a) - a \cosh(r_a)] \sin(\kappa z) \\
&\quad - [b \cosh(r_b) - b^\dagger e^{i\mu_b} \sinh(r_b)] \cos(\kappa z).
\end{aligned} \quad \text{(A1b)}
$$

With this, the single-mode quadrature variances $\langle (\Delta X_j)^2 \rangle$ can be written as

$$
\begin{aligned}
\langle (\Delta X_1^a)^2 \rangle = \tfrac{1}{4}[&-\cos^2(\kappa z) \sinh(2r_a) \cos(\mu_a) \\
&+ \sin^2(\kappa z) \sinh(2r_b) \cos(\mu_b) \\
&+ \cos^2(\kappa z) \cosh(2r_a) + \sin^2(\kappa z) \cosh(2r_b)],
\end{aligned}
$$
$$
\text{(A2a)}
$$

$$
\begin{aligned}
\langle (\Delta X_2^a)^2 \rangle = \tfrac{1}{4}[&\cos^2(\kappa z) \sinh(2r_a) \cos(\mu_a) \\
&- \sin^2(\kappa z) \sinh(2r_b) \cos(\mu_b) \\
&+ \cos^2(\kappa z) \cosh(2r_a) + \sin^2(\kappa z) \cosh(2r_b)].
\end{aligned}
$$
$$
\text{(A2b)}
$$

These variances are the same for the second waveguide (mode b). For the particular case of $\xi_a = \xi_b$ real ($\mu_a = \mu_b = 0$), Eqs. (A2) reduce to $(1/4)[\cosh^2(2r_a) - \sinh(2r_a)\cos(2\kappa z)]$, plotted in the cyan curves in Fig. 2(b).

APPENDIX B: INJECTION OF A TWO-MODE SQUEEZED STATE TO THE OPTICAL DIMER

In the case of injecting a sole two-mode squeezed state to the system with two input and two output ports, the input state can be written as $|\psi_0'\rangle = S_{ab}|0,0\rangle$, with $S_{ab} = \exp\{(\chi a^\dagger b^\dagger - \chi^* ab)\}$ and $\chi = r_{ab} \exp i\mu_{ab}$. Then, the evolu-

tion of the state $|\psi\rangle = U^{-1} S_{ab} U|0,0\rangle$ has the form

$$
|\psi\rangle = \exp\{\phi_a^* a + \phi_b^* b + \phi_{ab} a^\dagger b^\dagger - \text{H.c.}\}|0,0\rangle \quad \text{(B1)}
$$

with

$$
\phi_a = \chi e^{i\delta} \cos(\theta) \sin(\theta), \quad \text{(B2a)}
$$

$$
\phi_b = -\chi e^{-i\delta} \cos(\theta) \sin(\theta), \quad \text{(B2b)}
$$

$$
\phi_{ab} = \chi [\cos^2(\theta) - \sin^2(\theta)]. \quad \text{(B2c)}
$$

It is clear from the above expressions that in order to generate single-mode squeezed states $\phi_{ab} = 0$, which implies that $\theta = \pi/4$. Then, $\phi_a = \chi \exp i\delta/2$ and $\phi_b = -\chi \exp -i\delta/2$. A sole two-mode squeezed state will be recovered for $\theta = (2n + 1)\pi/2$ or $\theta = n\pi$. This general result is valid for the optical dimer with $\delta = \pi/2$ and $\theta = \kappa z$.

APPENDIX C: THREE-MODE SQUEEZING IN AN OPTICAL TRIMER: GENERAL CASE

As we see in Sec. III, an optical system with three input and three output ports can generate a state with mixed characteristics between three uncoupled single-mode squeezed states and a sole three-mode squeezed state

$$
\begin{aligned}
|\Psi\rangle_T = \exp\Big\{ &\tfrac{1}{2}(T_a^* a^2 + T_b^* b^2 + T_c^* c^2 + T_{ab} a^\dagger b^\dagger \\
&+ T_{ac} a^\dagger c^\dagger + T_{bc} b^\dagger c^\dagger - \text{H.c.})\Big\}|0,0,0\rangle.
\end{aligned} \quad \text{(C1)}
$$

This state can be generated by

$$
|\Psi\rangle_T = U_T^{-1} S_a S_b S_c U_T |0,0,0\rangle, \quad \text{(C2)}
$$

where S_j are single-mode squeezing operators for j different modes while U represents a unitary rotation operator that coherently mixes the three modes a, b, and c,

$$
U_T = \exp\{(\alpha^* ab^\dagger - \alpha ba^\dagger + \beta^* bc^\dagger - \beta cb^\dagger)\}, \quad \text{(C3)}
$$

with $\alpha = \theta_\alpha e^{i\delta_\alpha}$ and $\beta = \theta_\beta e^{i\delta_\beta}$ complex numbers. This is the most general expression for such a rotation. In order to obtain an analytical expression of (C1), we need to calculate $U_T^{-1} a U_T$, $U_T^{-1} b U_T$, and $U_T^{-1} c U_T$. We use the recursive notation $[A, B]_n = [A, [A, B]_{n-1}]$, where for $n = 1$, and we define $[A, B]_1 = [A, B]$, to write the Baker-Campbell-Hausdorff formula as

$$
e^A B e^{-A} = B + \sum_{n=1}^{\infty} \frac{[A, B]_n}{n!}. \quad \text{(C4)}
$$

Given Eqs. (C2) and (C3), the operator A is

$$
A = \alpha^* ab^\dagger - \alpha a^\dagger b + \beta^* bc^\dagger - \beta b^\dagger c, \quad \text{(C5)}
$$

and the commutative relations that we need to calculate are

$$
[A, a] = \alpha b, \quad \text{(C6)}
$$

$$
[A, b] = \beta c - \alpha^* a, \quad \text{(C7)}
$$

$$
[A, c] = -\beta^* b. \quad \text{(C8)}
$$

Defining $\lambda^2 = |\alpha|^2 + |\beta|^2$ we get for $\alpha \neq \beta$

$$U_T^{-1} a U_T = \left[1 - 2\frac{\theta_\alpha^2}{\lambda^2} \sin^2\left(\frac{\lambda}{2}\right) \right] a + \frac{\theta_\alpha}{\lambda} e^{i\delta_\alpha} \sin(\lambda) b + 2\frac{\theta_\alpha \theta_\beta}{\lambda^2} e^{i(\delta_\alpha + \delta_\beta)} \sin^2\left(\frac{\lambda}{2}\right) c,$$

$$U_T^{-1} b U_T = -\frac{\theta_\alpha}{\lambda} e^{-i\delta_\alpha} \sin(\lambda) a + \cos(\lambda) b + \frac{\theta_\beta}{\lambda} e^{i\delta_\beta} \sin(\lambda) c,$$

$$U_T^{-1} c U_T = 2\frac{\theta_\alpha \theta_\beta}{\lambda^2} e^{-i(\delta_\alpha + \delta_\beta)} \sin^2\left(\frac{\lambda}{2}\right) a - \frac{\theta_\beta}{\lambda} e^{-i\delta_\beta} \sin(\lambda) b + \left[1 - 2\frac{\theta_\beta^2}{\lambda^2} \sin^2\left(\frac{\lambda}{2}\right) \right] c.$$

In the particular case of $|\alpha| = |\beta| = \theta$, and $\delta_\alpha = \delta_\beta = \delta$, i.e., the same coupling between waveguides a and b and b and c, we can reduce the above expressions to

$$U_T^{-1} a U_T = \cos^2\left(\frac{\theta}{\sqrt{2}}\right) a + \frac{e^{i\delta}}{\sqrt{2}} \sin(\sqrt{2}\theta) b + e^{2i\delta} \sin^2\left(\frac{\theta}{\sqrt{2}}\right) c,$$

$$U_T^{-1} b U_T = -\frac{1}{\sqrt{2}} e^{-i\delta} \sin(\sqrt{2}\theta) a + \cos(\sqrt{2}\theta) b + \frac{1}{\sqrt{2}} e^{i\delta} \sin(\sqrt{2}\theta) c,$$

$$U_T^{-1} c U_T = e^{-2i\delta} \sin^2\left(\frac{\theta}{\sqrt{2}}\right) a - \frac{1}{\sqrt{2}} e^{-i\delta} \sin(\sqrt{2}\theta) b + \cos^2\left(\frac{\theta}{\sqrt{2}}\right) c.$$

Using these results and calculating $U_T^\dagger u^2 U_T$ and $U_T^\dagger u^{\dagger 2} U_T$, with $u = a, b, c$, we find the following T_i and T_{ij} coefficients for $\alpha \neq \beta$:

$$T_a = \xi_a \left[1 - 2\frac{\theta_\alpha^2}{\lambda^2} \sin^2\left(\frac{\lambda}{2}\right) \right]^2 + \xi_b \frac{\theta_\alpha^2}{\lambda^2} e^{2i\delta_\alpha} \sin^2(\lambda) + \xi_c 4 \frac{\theta_\alpha^2 \theta_\beta^2}{\lambda^4} e^{2i(\delta_\alpha + \delta_\beta)} \sin^4\left(\frac{\lambda}{2}\right),$$

$$T_b = \xi_a \frac{\theta_\alpha^2}{\lambda^2} e^{-2i\delta_\alpha} \sin^2(\lambda) + \xi_b \cos^2(\lambda) + \xi_c \frac{\theta_\beta^2}{\lambda^2} e^{2i\delta_\beta} \sin^2(\lambda),$$

$$T_c = \xi_a 4 \frac{\theta_\alpha^2 \theta_\beta^2}{\lambda^4} e^{-2i(\delta_\alpha + \delta_\beta)} \sin^4\left(\frac{\lambda}{2}\right) + \xi_b \frac{\theta_\beta^2}{\lambda^2} e^{-2i\delta_\beta} \sin^2(\lambda) + \xi_c \left[1 - 2\frac{\theta_\beta^2}{\lambda^2} \sin^2\left(\frac{\lambda}{2}\right) \right]^2,$$

$$T_{ab} = -\left\{ \xi_a 2 \frac{\theta_\alpha}{\lambda} e^{-i\delta_\alpha} \left[1 - 2\frac{\theta_\alpha^2}{\lambda^2} \sin^2\left(\frac{\lambda}{2}\right) \right] \sin(\lambda) - \xi_b \frac{\theta_\alpha}{\lambda} e^{i\delta_\alpha} \sin(2\lambda) - \xi_c 4 \frac{\theta_\alpha \theta_\beta^2}{\lambda^3} e^{i(\delta_\alpha + 2\delta_\beta)} \sin(\lambda) \sin^2\left(\frac{\lambda}{2}\right) \right\}, \tag{C9}$$

$$T_{ac} = -\left\{ \xi_a 4 \frac{\theta_\alpha \theta_\beta}{\lambda^2} e^{-i(\delta_\alpha + \delta_\beta)} \left[1 - 2\frac{\theta_\alpha^2}{\lambda^2} \sin^2\left(\frac{\lambda}{2}\right) \right] \sin^2\left(\frac{\lambda}{2}\right) - \xi_b 2 \frac{\theta_\alpha \theta_\beta}{\lambda^2} e^{i(\delta_\alpha - \delta_\beta)} \sin^2(\lambda) \right.$$
$$\left. + \xi_c 4 \frac{\theta_\alpha \theta_\beta}{\lambda^2} e^{i(\delta_\alpha + \delta_\beta)} \left[1 - 2\frac{\theta_\beta^2}{\lambda^2} \sin^2\left(\frac{\lambda}{2}\right) \right] \sin^2\left(\frac{\lambda}{2}\right) \right\},$$

$$T_{bc} = -\left\{ \xi_a 4 \frac{\theta_\alpha^2 \theta_\beta}{\lambda^3} e^{-i(2\delta_\alpha + \delta_\beta)} \sin(\lambda) \sin^2\left(\frac{\lambda}{2}\right) + \xi_b \frac{\theta_\beta}{\lambda} e^{-i\delta_\beta} \sin(2\lambda) - \xi_c 2 \frac{\theta_\beta}{\lambda} e^{i\delta_\beta} \left[1 - 2\frac{\theta_\beta^2}{\lambda^2} \sin^2\left(\frac{\lambda}{2}\right) \right] \sin(\lambda) \right\}.$$

For equal coupling ($\alpha = \beta$), we obtain the following simplified expressions:

$$T_a = \xi_a \cos^4\left(\frac{\theta}{\sqrt{2}}\right) + \xi_b \frac{1}{2} e^{2i\delta} \sin^2(\sqrt{2}\theta) + \xi_c e^{4i\delta} \sin^4\left(\frac{\theta}{\sqrt{2}}\right),$$

$$T_b = \xi_a \frac{1}{2} e^{-2i\delta} \sin^2(\sqrt{2}\theta) + \xi_b \cos^2(\sqrt{2}\theta) + \xi_c \frac{1}{2} e^{2i\delta} \sin^2(\sqrt{2}\theta),$$

$$T_c = \xi_c e^{-4i\delta} \sin^4\left(\frac{\theta}{\sqrt{2}}\right) + \xi_b \frac{1}{2} e^{-2i\delta} \sin^2(\sqrt{2}\theta) + \xi_c \cos^4\left(\frac{\theta}{\sqrt{2}}\right),$$

$$T_{ab} = -\left\{ \xi_a \sqrt{2} e^{-i\delta} \sin(\sqrt{2}\theta) \cos^2\left(\frac{\theta}{\sqrt{2}}\right) - \xi_b \frac{1}{\sqrt{2}} e^{i\delta} \sin(2\sqrt{2}\theta) - \xi_c \sqrt{2} e^{3i\delta} \sin(\sqrt{2}\theta) \sin^2\left(\frac{\theta}{\sqrt{2}}\right) \right\}, \tag{C10}$$

$$T_{ac} = -\left\{ \xi_a \frac{1}{2} e^{-2i\delta} \sin^2(\sqrt{2}\theta) - \xi_b \sin^2(\sqrt{2}\theta) + \xi_c \frac{1}{2} e^{2i\delta} \sin^2(\sqrt{2}\theta) \right\},$$

$$T_{bc} = -\left\{ \xi_a \sqrt{2} e^{-i3\delta} \sin(\sqrt{2}\theta) \sin^2\left(\frac{\theta}{\sqrt{2}}\right) + \xi_b \frac{1}{\sqrt{2}} e^{-i\delta} \sin(2\sqrt{2}\theta) - \xi_c \sqrt{2} e^{i\delta} \sin(\sqrt{2}\theta) \cos^2\left(\frac{\theta}{\sqrt{2}}\right) \right\}.$$

These are the coefficients that lead to Eq. (21) in the main text when making $\delta = \pi/2$.

[1] V. Giovannetti, S. Lloyd, and L. Maccone, Advances in quantum metrology, Nat. Photonics **5**, 222 (2011).

[2] R. Loudon and P. L. Knight, Squeezed light, J. Mod. Opt. **34**, 709 (1987).

[3] K. Fukui, A. Tomita, A. Okamoto, and K. Fujii, High-Threshold Fault-Tolerant Quantum Computation with Analog Quantum Error Correction, Phys. Rev. X **8**, 021054 (2018).

[4] W. Ge, B. C. Sawyer, J. W. Britton, K. Jacobs, J. J. Bollinger, and M. Foss-Feig, Trapped Ion Quantum Information Processing with Squeezed Phonons, Phys. Rev. Lett. **122**, 030501 (2019).

[5] M. Davanco, J. Liu, L. Sapienza, C.-Z. Zhang, J. V. De Miranda Cardoso, V. Verma, R. Mirin, S. W. Nam, L. Liu, and K. Srinivasan, Heterogeneous integration for on-chip quantum photonic circuits with single quantum dot devices, Nat. Commun. **8**, 889 (2017).

[6] A. Crespi, M. Lobino, J. C. F. Matthews, A. Politi, C. R. Neal, R. Ramponi, R. Osellame, and J. L. O'Brien, Measuring protein concentration with entangled photons, Appl. Phys. Lett. **100**, 233704 (2012).

[7] J. Aasi *et al.*, Enhanced sensitivity of the ligo gravitational wave detector by using squeezed states of light, Nat. Photonics **7**, 613 (2013).

[8] M. Gessner, L. Pezzè, and A. Smerzi, Sensitivity Bounds for Multiparameter Quantum Metrology, Phys. Rev. Lett. **121**, 130503 (2018).

[9] L. Pezzè, M. A. Ciampini, N. Spagnolo, P. C. Humphreys, A. Datta, I. A. Walmsley, M. Barbieri, F. Sciarrino, and A. Smerzi, Optimal Measurements for Simultaneous Quantum Estimation of Multiple Phases, Phys. Rev. Lett. **119**, 130504 (2017).

[10] S. Ragy, M. Jarzyna, and R. Demkowicz-Dobrzański, Compatibility in multiparameter quantum metrology, Phys. Rev. A **94**, 052108 (2016).

[11] A. S. Coelho, F. A. S. Barbosa, K. N. Cassemiro, A. S. Villar, M. Martinelli, and P. Nussenzveig, Three-color entanglement, Science **326**, 823 (2009).

[12] I. V. Sokolov and M. I. Kolobov, Squeezed-light source for superresolving microscopy, Opt. Lett. **29**, 703 (2004).

[13] C. Simon, H. de Riedmatten, M. Afzelius, N. Sangouard, H. Zbinden, and N. Gisin, Quantum Repeaters with Photon Pair Sources and Multimode Memories, Phys. Rev. Lett. **98**, 190503 (2007).

[14] L.-M. Duan, M. D. Lukin, J. I. Cirac, and P. Zoller, Long-distance quantum communication with atomic ensembles and linear optics, Nature (London) **414**, 413 (2001).

[15] Brian E. Anderson, Prasoon Gupta, Bonnie L. Schmittberger, Travis Horrom, Carla Hermann-Avigliano, Kevin M. Jones, and Paul D. Lett, Phase sensing beyond the standard quantum limit with a variation on the su(1, 1) interferometer, Optica **4**, 752 (2017).

[16] F. Wen, Z. Li, Y. Zhang, H. Gao, J. Che, J. Che, H. Abdulkhaleq, Y. Zhang, and H. Wang, Triple-mode squeezing with dressed six-wave mixing, Sci. Rep. **6**, 25554 (2016).

[17] C. Kittel, *Introduction to Solid State Physics*, 7th ed. (Wiley, New York, 1996).

[18] J. D. Joannopoulos *et al.*, *Photonic Crystals: Molding the Flow of Light*, 2nd ed. (Princeton University Press, Princeton, NJ, 2008).

[19] A. Rai, G. S. Agarwal, and J. H. H. Perk, Transport and quantum walk of nonclassical light in coupled waveguides, Phys. Rev. A **78**, 042304 (2008).

[20] B. M. Rodríguez-Lara, Propagation of nonclassical states of light through one-dimensional photonic lattices, J. Opt. Soc. Am. B **31**, 878 (2014).

[21] S. Longhi, Optical Bloch Oscillations and Zener Tunneling with Nonclassical Light, Phys. Rev. Lett. **101**, 193902 (2008).

[22] H. Tang, X.-F. Lin, Z. Feng, J.-Y. Chen, J. Gao, K. Sun, C.-Y. Wang, P.-C. Lai, X.-Y. Xu, Y. Wang, L.-F. Qiao, A.-L. Yang, and X.-M. Jin, Experimental two-dimensional quantum walk on a photonic chip, Sci. Adv. **4**, eaat3174 (2018).

[23] A. Peruzzo, M. Lobino, J. C. F. Matthews, N. Matsuda, A. Politi, K. Poulios, X.-Q. Zhou, Y. Lahini, N. Ismail, K. Wörhoff, Y. Bromberg, Y. Silberberg, M. G. Thompson, and J. L. O'Brien, Quantum walks of correlated photons, Science **329**, 1500 (2010).

[24] H. E. Kondakci, A. F. Abouraddy, and B. E. A. Saleh, Lattice topology dictates photon statistics, Sci. Rep. **7**, 8948 (2017); A photonic thermalization gap in disordered lattices, Nat. Phys. **11**, 930 (2015); H. E. Kondakci, A. Szameit, A. F. Abouraddy, D. N. Christodoulides, and B. E. A. Saleh, Interferometric control of the photon-number distribution, APL Photonics **2**, 071301 (2017).

[25] A. Aspuru-Guzik and P. Walther, Photonic quantum simulators, Nat. Phys. **8**, 285 (2012).

[26] G. Yeoman and S. M. Barnett, Two-mode squeezed Gaussons, J. Mod. Opt. **40**, 1497 (1993).

[27] S. Rojas-Rojas, L. Morales-Inostroza, R. A. Vicencio, and A. Delgado, Quantum localized states in photonic flat-band lattices, Phys. Rev. A **96**, 043803 (2017).

[28] B. R. Mollow, Quantum statistics of coupled oscillator systems, Phys. Rev. **162**, 1256 (1967).

[29] L. E. Estes, T. H. Keil, and L. M. Narducci, Quantum-mechanical description of two coupled harmonic oscillators, Phys. Rev. **175**, 286 (1968).

[30] A. Marino, Experimental studies of two-mode squeezed states in rubidium vapor, Ph.D. thesis, The Institute of Optics, The College School of Engineering and Applied Sciences, University of Rochester, Rochester, New York, 2006.

[31] S. Haroche and J. M. Raimond, *Exploring the Quantum: Atoms, Cavities, and Photons* (Oxford University Press, Oxford, 2013).

[32] S. L. Braunstein and P. van Loock, Quantum information with continuous variables, Rev. Mod. Phys. **77**, 513 (2005).

[33] T. Das, R. Prabhu Aditi Sen(De), and U. Sen, Superiority of photon subtraction to addition for entanglement in a multimode squeezed vacuum, Phys. Rev. A **93**, 052313 (2016).

[34] A. Peres, Separability Criterion for Density Matrices, Phys. Rev. Lett. **77**, 1413 (1996).

[35] P. Horodecki, Separability criterion and inseparable mixed states with positive partial transposition, Phys. Lett. A **232**, 333 (1997).

[36] R. Simon, Peres-Horodecki Separability Criterion for Continuous Variable Systems, Phys. Rev. Lett. **84**, 2726 (2000).

[37] Zh. Qin, M. Gessner, Zh. Ren, X. Deng, D. Han, W. Li, X. Su, A. Smerzi, and K. Peng, Characterizing the multipartite continuous-variable entanglement structure from squeezing coefficients and the Fisher information, npj Quantum Inf. **5**, 3 (2019).

[38] S. Armstrong, M. Wang, R. Y. Teh, Q. Gong, Q. He, J. Janousek, H.-A. Bachor, M. D. Reid, and P. K. Lam, Multipartite Einstein-Podolsky-Rosen steering and genuine tripartite entanglement with optical networks, Nat. Phys. **11**, 167 (2015).

[39] L. K. Shalm, D. R. Hamel, C. Simon, Z. Yan, K. J. Resch, and T. Jennewein, Three-photon energytime entanglement, Nat. Phys. **9**, 19 (2013).

[40] G. Giedke, B. Kraus, M. Lewenstein, and J. I. Cirac, Separability properties of three-mode Gaussian states, Phys. Rev. A **64**, 052303 (2001).

[41] A. Szameit, F. Dreisow, Th. Pertsch, S. Nolte, and A. Tünnermann, Control of directional evanescent coupling in fs laser written waveguides, Opt. Express **15**, 1579 (2007).

[42] S. Rojas-Rojas, M. Morales-Inostroza, U. Naether, G. B. Xavier, S. Nolte, A. Szameit, R. A. Vicencio, G. Lima, and A. Delgado, Analytical model for polarization-dependent light propagation in waveguide arrays and applications, Phys. Rev. A **90**, 063823 (2014).

[43] L. Mandel and E. Wolf, *Optical Coherence and Quantum Optics*, 1st ed. (Cambridge University Press, New York, 1995).

[44] M. A. Nielsen and I. L. Chuang, *Quantum Computation and Quantum Information*, 10th anniversary edition (Cambridge University Press, Cambridge, 2010).

[45] D. Blömer, A. Szameit, F. Dreisow, Th. Schreiber, S. Nolte, and A. Tünnermann, Nonlinear refractive index of fs-laser-written waveguides in fused silica, Opt. Express **14**, 2151 (2006).